The College of Engineering
University of Wisconsin-Madison

Wisconsin Electric Machines and Power Electronics Consortium

RESEARCH REPORT
90-29

Characterization of GTOs Under Different Modes of Zero Current Switching

P. Caldeira, T. A. Lipo
Dept. of Elec. and Comp. Engr.
University of Wisconsin-Madison
1415 Johnson Drive
Madison, WI 53706-1691

A. Mertens, H.-Ch. Skudelny
Inst. for Power Elect. & Elec. Drives
RWTH Aachen University of Tech.
Jägerstraße 17/19
5100 Aachen West Germany

WEMPEC

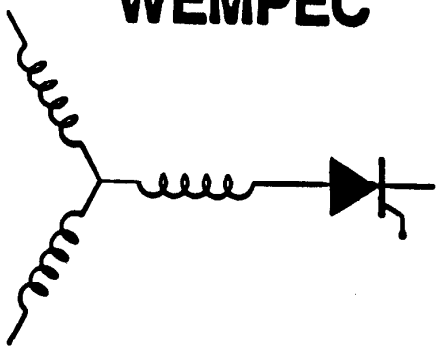

Department of Electrical and Computer Engineering
1415 Johnson Drive
Madison, Wisconsin 53706

CHARACTERIZATION OF GTOS UNDER DIFFERENT MODES OF ZERO CURRENT SWITCHING

A. Mertens and H.-Ch. Skudelny
Institute for Power Electronics and Electrical Drives
RWTH Aachen University of Technology
Jägerstraße 17/19, 5100 Aachen
West Germany

P. Caldeira and T. Lipo
Dept. of Electrical and Computer Engineering
University of Wisconsin-Madison
1415 Johnson Drive
Madison, Wisconsin 53706

Abstract

In recent years, several papers appeared describing the use of GTOs in zero current switching applications, with the goal of increasing the frequency range for medium to high power converters.

Zero current switching with GTOs can be applied in series and parallel resonant converters, as well as PWM inverters with commutation aid networks. The voltage and current waveforms at the devices differ in each of these applications, and different modes of Zero Current Switching (ZCS) can be identified. In this paper, a comparative view of the behaviour and characteristics of the GTO in the different modes of ZCS is presented.

The variety of ZCS waveforms is described and transferred into a unifying schematic. The behaviour of GTOs in the different modes of operation is characterized, and requirements to the circuit environment are pointed out. The relations between the most important circuit parameters and some of the device waveform parameters are investigated experimentally.

1 Introduction

At the high end of the power range of today's power electronic equipment, the thyristor and the GTO are still the only devices applicable. The switching frequencies used for generation and control of DC or sinusoidal output voltages and currents are restricted to a few hundred Hertz because of the large turn-off time in thyristor circuits, and the very high switching losses of GTOs. The same characteristics limit the frequency of high power resonant inverters which are mainly used in induction heating applications.

A successful approach to reduce the turn-off time of thyristors was made with the gate-assisted turn-off mode (GATO). With a negative gate voltage applied during the hold-off time, the device can be held in the off state when positive voltage is reapplied, even if a forward recovery current occurs due to the presence of remaining carriers in the central regions of the device. This current is deviated into the gate instead of flowing via the gate cathode junction and turning on the device. The effectiveness of this method depends on the gate structure. The turn-off time could be reduced significantly, but not below about 8 microseconds.

It is obvious that the GTO with its much finer gate structure is ideally suited for the gate-assisted turn-off mode, and promises even lower turn-off times and higher frequencies. Several papers appeared in recent years describing the use of GTOs in zero current switching applications [1], [2], [5]-[7], [9]-[12]. Some device manufacturers even announced an optimized GTO-like device for such applications, the Zero Turn-Off Time Thyristor (ZTO) [3], [4].

Zero current switching with GTOs can be applied in all circuits where thyristors have been used so far. The voltage and current waveforms at the devices differ in many of the applications, and so does the device behaviour. Several different modes of zero current switching (ZCS) can be identified.

The characteristics of GTOs under ZCS are much different from the characteristics under normal GTO operation. They also differ from a normal thyristor behaviour, because of the different device design (doping, gate structure) and the negative gate voltage applied for turn-off.

This paper gives a comparative view of the different modes of ZCS with GTOs. The variety of ZCS waveforms is described and transferred into a unifying schematic. The behaviour of GTOs in the different modes of operation is characterized and evaluated, and requirements to the circuit environment and operation conditions are

pointed out. The relations between the most important circuit parameters and some device characteristics are investigated experimentally.

2 Modes of Zero Current Switching Operation

The GTO can be applied in ZCS modes of operation wherever a thyristor can be used. This includes choppers and PWM inverters with commutation aid networks [6], [7], as well as series and parallel resonant converters [1], [2], [9]-[12]. A new ZCS circuit for UPS and drive applications,

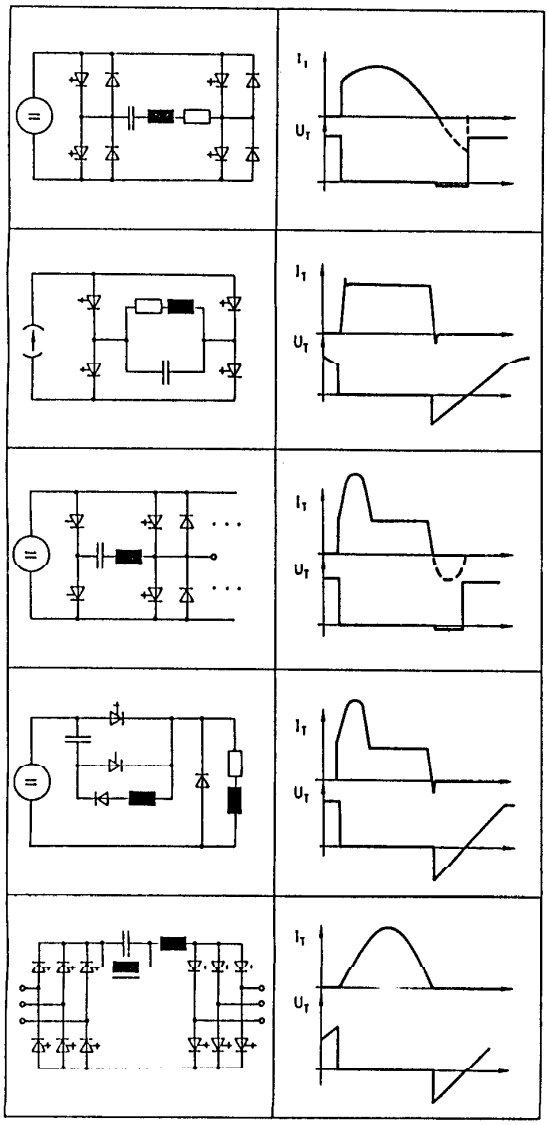

Figure 1: Different circuits where GTOs can be applied in a ZCS mode of operation: series resonant inverter, parallel resonant converter, PWM inverter and chopper using forced commutation and resonant DC current link inverter

the resonant DC current link inverter (RDCCLI) has been introduced in reference [8], where high switching frequencies are necessary for acceptable output waveforms because of the discrete nature of the current pulses. Figure 1 shows all of the circuits mentioned above and their basic waveforms.

The different waveforms can be divided into four basic modes of operation (fig. 2). The current is shaped either sinusoidal (series resonant inverter, resonant DC current link inverter) or trapezoidal (voltage pulse commutation, current pulse commutation, parallel resonant converter). The voltage is either a ramp, starting with negative values (parallel resonant converter, voltage pulse commutation), or it is only slightly negative during the hold-off time and jumps to a forward blocking voltage afterwards (all the applications with an antiparallel diode, like series resonant inverter and current pulse commutation). All of the four possible combinations appear in the circuits of fig. 1.

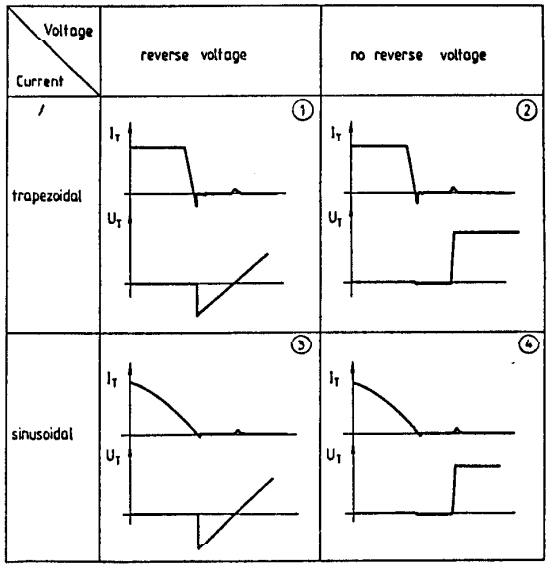

Figure 2: Basic modes of zero current switching

3 Behaviour of GTOs in Zero Current Switching

General Considerations

On principle, the GTO has a structure similar to a thyristor. Some variations in the design are made in order to achieve gate turn-off capability. This concerns both the gate structure, which has to be highly interdigitated with the cathode, and some precautions to reduce the base transport coefficient of the anode-side pnp

transistor, in order to achieve a reasonable turn-off gain. These precautions include the implementation of anode shortings or a heavy gold doping of the thick n-base of the GTO. Both measures result in a reduction of the stored charge inside the n-base.

The gate is designed so that charge can be extracted from the p- and n-base via the gate, and that all of the area covered by the cathode can be evacuated very quickly. This and the reduced amount of charge in the base regions is advantageous for a very short turn-off time in ZCS operation. Therefore the switching behaviour of the GTO in ZCS should compare favourable to a similarly rated conventional thyristor.

For some of the ZCS modes in fig. 2, reverse blocking switches have to be used. In an anode shorted GTO, the reverse blocking junction is shorted out. Only gold-doped devices can be used in these applications, as far as no diode is connected in series to the GTO.

It has been shown in previous papers [1], [7], [9] that for very short hold-off times in ZCS with reverse voltage, it may be necessary to use a switch as shown in fig. 3 instead of a single GTO, even if the GTO is of the reverse blocking type. If the GTO is brought from the on state to the reverse blocking state very quickly, the remaining stored charge is trapped between two blocking junctions and can be removed only by recombination. The central junction is still forward biased in this situation. During the transition from the reverse blocking to the forward blocking state, a forward recovery current will occur that removes the stored charge from the central junction and thus makes it reverse biased. This forward recovery current can cause the GTO to turn on if the gate drive is not capable to absorb it completely.

The switch in fig. 3 avoids that the GTO has to block reverse voltage, and thus the central junction can be brought to a reverse biased state before the switch has to sustain a forward blocking voltage.

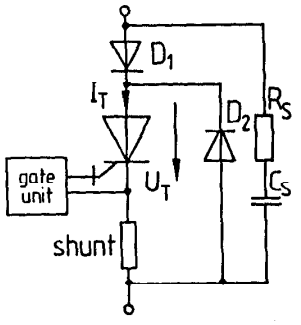

Figure 3: Improved GTO switch for use in ZCS with reverse blocking voltage

Test Circuits

The switching behaviour of GTOs in zero current switching applications was investigated experimentally. A number of test circuits was used to simulate the different modes of ZCS in a single shot mode. The circuits are shown in fig. 4. A GTO 160PFT160 (1600 V, 600 A) was used in all the tests at a current of 300 A peak.

The two circuits at the top of fig. 4 are used for trapezoidal current waveforms. When T_1 is turned on, the current in L_d and T_1 rises slowly. When the specified value is reached, T_2 is turned on. The current commutates to T_2, and T_1 is turned off in a ZCS mode. If the GTO is used alone or with a series and antiparallel diode,

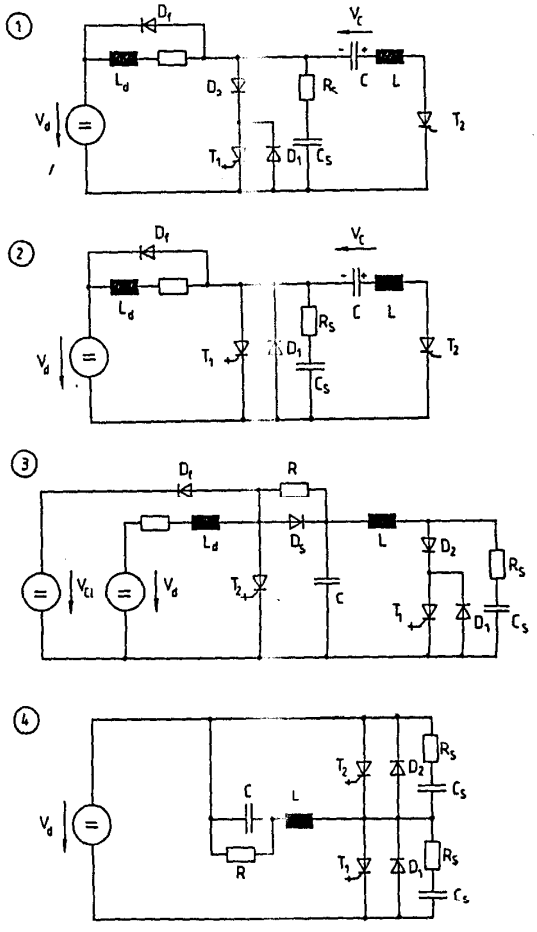

Figure 4: Test circuits used to simulate the switching waveforms in the different ZCS modes

the voltage V_c appears as a reverse blocking voltage across T_1 or D_2. Then V_c is rising linearly until it equals V_d. This corresponds to mode 1 in fig. 2. If the GTO is used with an antiparallel diode as shown in the second circuit of fig. 4, the resonance between L and C continues until D_1 blocks. At this time, V_c has changed polarity and appears suddenly across T_1 as a forward blocking voltage. Thus mode 2 in fig. 2 is also simulated. The component values are V_d = 540 V, L_d = 1 mH. L and C were varied from 2.6 µH to 8.9 µH and from 4.7 µF to 10.2 µF, respectively. V_c was also varied between 300 V and 500 V. Thus different waveform parameters such as dI/dt, dV/dt, tq, V_{rm} could be adjusted.

The third circuit in fig. 4 simulates the waveforms obtained in ZCS mode 3 in fig. 2. The component values are V_d = 150 V, V_{Cl} = 500 V, L_d = 1 mH, C = 2.7 µF and L = 20 µH. First T_2 is turned on to build up a current in L_d of approximately 150 A. When T_2 is turned off at $t = t_0$, L_d acts as a current source, and the voltage across C rises linearly until GTO T_1 is turned on at $t = t_1$. Now a resonant current pulse of the shape

$$I_L = I_{Ld} \cdot (1-\cos\omega t) + \sqrt{(C/L)} \cdot V_C(t_1) \cdot \sin\omega t, \qquad (1)$$

where $\omega = 1/\sqrt{LC}$, flows through L and T_1. When this current returns to zero, T_1 is turned off. Inbetween the polarity of V_C has reversed due to resonant discharge and appears as a reverse blocking voltage across T_1 and D_2. Due to the current source L_d, the voltage V_C rises linearly until it reaches V_{Cl}. With the above component values, an equivalent resonant pulse frequency of 20 kHz is obtained. The hold-off time can be adjusted by changing the capacitor charging time ($t_1 - t_0$).

The last circuit in fig. 4 simulates the waveforms of ZCS mode 4 in fig. 2. These waveforms are characteristic for a series resonant inverter. When T_1 is turned on, a sinusoidal current pulse flows through V_d, C, L, and T_1. When the current reverses, T_1 is turned off while D_1 starts conducting. The hold-off interval is terminated when T_2 is turned on and the voltage across T_1 rises very quickly to V_d. In this setup, V_d was 500 V and L and C were chosen to reach a current amplitude of 300 A at various values of the equivalent resonant frequency between 10 kHz and 25 kHz.

With these test circuits, the switching waveforms typical for a GTO in different modes of ZCS where obtained. A variety of waveform parameters could be adjusted such that an investigation of the relationships between the device characteristics and the waveform parameters became possible.

Switching Waveforms

The switching waveforms obtained with GTOs in different modes of ZCS are discussed in the following. Figure 5 shows the turn-off waveforms of a single GTO in ZCS mode 1, obtained in the first circuit of fig. 4.

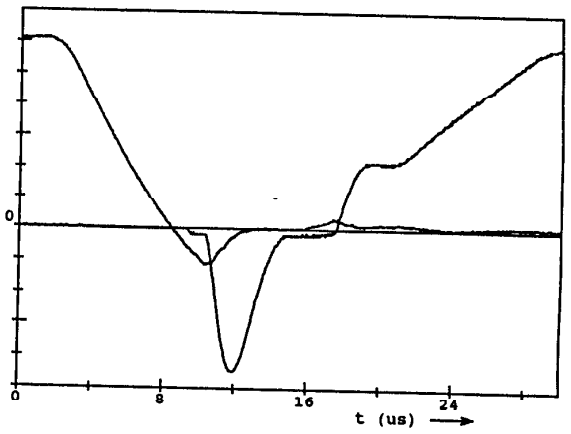

Figure 5: Turn-off waveforms of reverse blocking GTO in ZCS mode 1. I_T = 50 A/Div, V_T = 100 V/Div

After the anode current has fallen from its steady-state value (300 A) to zero, a reverse recovery current makes the gate-cathode junction block very soon, and the anode voltage jumps to the gate-cathode breakdown voltage. When the anode-side junction is also free of excess carriers, the anode voltage jumps to the commutation capacitor voltage. The step is smoothed by the RC snubber. The forward recovery process commences when the anode voltage has risen to zero. Now the anode current increases while the anode voltage remains zero until the central junction blocks. Then a step in anode voltage occurs, and afterwards the anode voltage rises linearly with the commutation capacitor voltage. During this time, a tail current is observed.

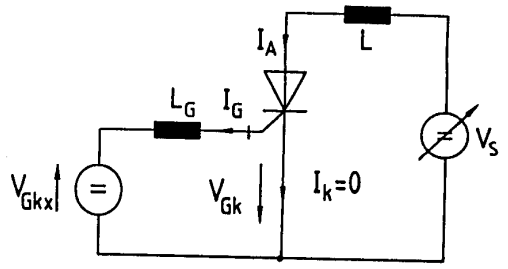

Figure 6: Equivalent circuit of the GTO and its environment during the forward recovery in ZCS modes 1 and 3

Figure 6 is used to discuss the operation conditions necessary for keeping the device in the off state during the forward recovery time. V_s is rising linearly at a rate dV_s/dt. A current flow starts when V_s equals $-V_{GKx}$. The anode current equals the gate current as long as $V_{GK} < 0$. If the gate-cathode voltage becomes positive, a cathode current may flow and may turn on the device.

The analysis of this circuit reveals that the device can be held in the off state when

$$\frac{dV_s}{dt} \leq \sqrt{\frac{V_{GKx}^3 \cdot (L + L_G)^2}{6 \cdot Q_f \cdot L_G^3}} \qquad (2)$$

where Q_f is the forward recovery charge that has to be removed from the central junction in order to attain blocking capability. Q_f depends on many parameters like the on-state current, the reverse recovery current, the hold-off time and the recombination time constant. For a certain operation condition, Q_f can be measured via the forward recovery current amplitude I_{fr} using the equation

$$Q_f = \frac{1}{6} \sqrt{\frac{8 \cdot I_{fr}^3 \cdot (L + L_G)}{dV_s/dt}} \; . \qquad (3)$$

In this mode of operation, losses occur during the reverse recovery, forward recovery and tail time.

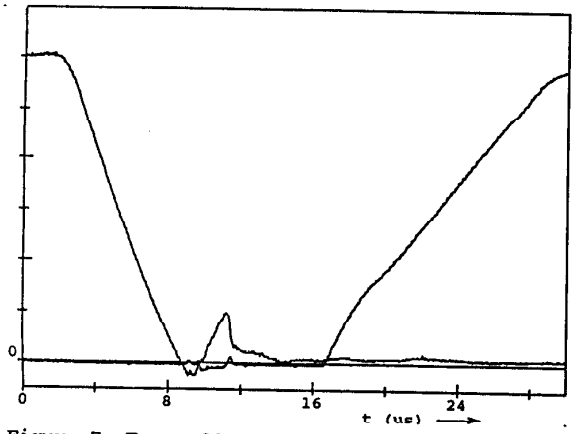

Figure 7: Turn-off waveforms of a GTO in a switch according to fig. 3 (ZCS mode 1). I_T = 50 A/Div, V_T = 100 V/Div

Figure 7 is showing the turn-off waveforms in the same circuit, but using a switch as shown in fig. 3 instead of a single GTO. Now the reverse voltage is blocked by the series diode, and the reverse recovery current of this diode is flowing through the antiparallel diode. During the hold-off time, the voltage across the GTO is zero. When the negative gate voltage is applied by the gate unit, the gate-cathode junction is blocking almost instantaneously because the cathode current is zero. The negative gate voltage is driving a current through the antiparallel diode, into the anode and out of the gate of the GTO. This current removes charge from the central junction and makes it reverse biased before the anode voltage rises. Turn-off losses occur only when the anode voltage is rising and are widely reduced as compared to conventional GTO operation because the tail current is reduced significantly [1], [7], [9].

In fig. 8, the switching waveforms obtained in the second circuit of fig. 4 are shown. They look quite similar to those in fig. 7, with the difference that the anode voltage rises very quickly after the hold-off time. As a result, the tail current is larger in the first few microseconds of the voltage risetime.

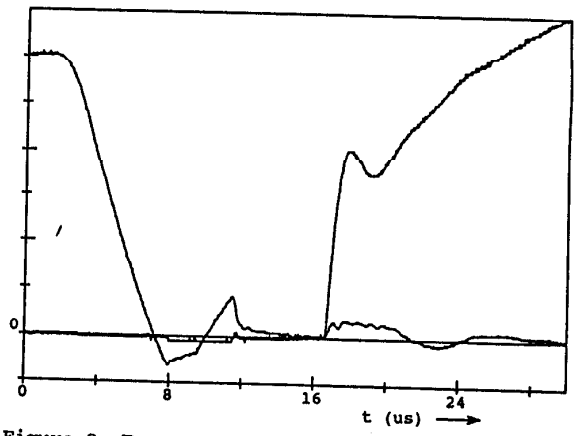

Figure 8: Turn-off waveforms of a GTO in ZCS mode 2. I_T = 50 A/Div, V_T = 100 V/Div

The next two figures show sinusoidal current waveforms of 300 A peak. In this case the excess carrier density inside the device cannot reach the same value as in the case of trapezoidal current of the same amplitude because the peak current is flowing only for a few microseconds. In addition, the stored charge has more time to recombine and to adjust to the lower currents during the current fall.

In the third circuit of fig. 4, a reverse blocking GTO could be used without series and antiparallel diodes because the large series inductance and the reduced stored charge make it easy to keep the device in the off-state during the forward recovery. However, the forward recovery time t_{fr} depends only slightly on L and Q_f:

$$t_{fr} = \sqrt[3]{\frac{6 \cdot Q_f \cdot (L + L_G)}{dV_s/dt}} \; . \qquad (4)$$

The time t_{fr} is adding to a minimum off time of the device that has to pass before the device can be turned on again. Especially in the RDCCLI, this is a major drawback because it increases all the component ratings of the circuit. Therefore it is advisible to use the switch configuration in fig. 3.

Figure 9 shows the turn-off waveforms obtained in the third circuit of fig. 4 when diodes are added to the GTO. The reduced amount of stored charge is visible in the reduced peak current during the hold-off time. Surprisingly there is almost no tail current when the anode voltage rises. Therefore the switching losses are very small in this application. The operating conditions in the RDCCLI seem to be very favourable for a GTO.

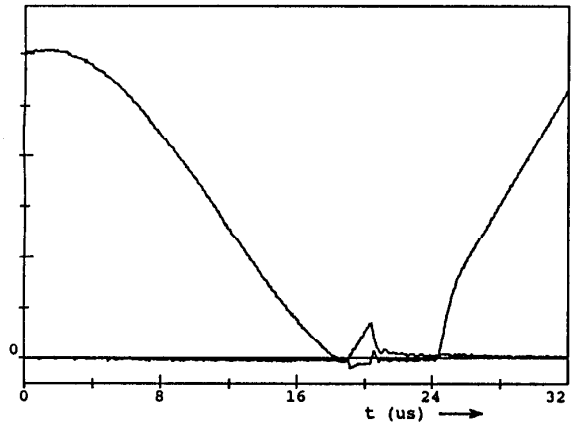

Figure 9: Turn-off waveforms of a GTO in a switch according to fig. 3 in ZCS mode 3. I_T = 50 A/Div, V_T = 100 V/Div

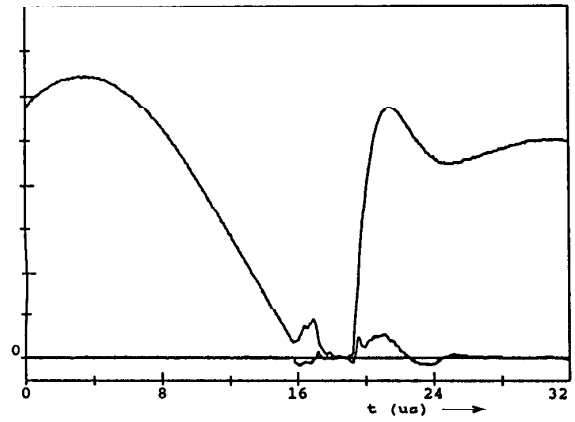

Figure 10: Turn-off waveforms of a GTO in ZCS mode 4. I_T = 50 A/Div, V_T = 100 V/Div

In fig. 10, the waveforms obtained in the last test circuit of fig. 4 are shown. It seems that the amount of stored charge is larger as compared to fig. 9, which may result from the steeper dI/dt. Since the voltage rises very quickly after the hold-off time, the tail current is much larger than in fig. 9 as was expected. However, a comparison to the ZCS modes 1 and 2 shows that the duration of the tail current is much shorter as a result of the sinusoidal current waveform and less charge to be removed. Therefore the losses can be expected to be much lower.

Investigation of Device Characteristics

Using the test circuits shown in fig. 4, some device characteristics were analyzed systematically. The investigation focused on the behaviour of a single GTO in ZCS mode 1, on the charge that has to be extracted via the gate during turn-off, and, most important, on the switching losses in the different ZCS modes.

The forward recovery current amplitude I_{Fr} of a reverse blocking GTO used in ZCS mode 1 is depicted in fig. 11 as a function of the hold-off interval t_q. As expected, I_{Fr} falls when t_q increases. This is a result of the recombination of excess carriers during t_q. It is also visible that a large series inductance L is important for keeping I_{Fr} within limits, as indicated by equation (3).

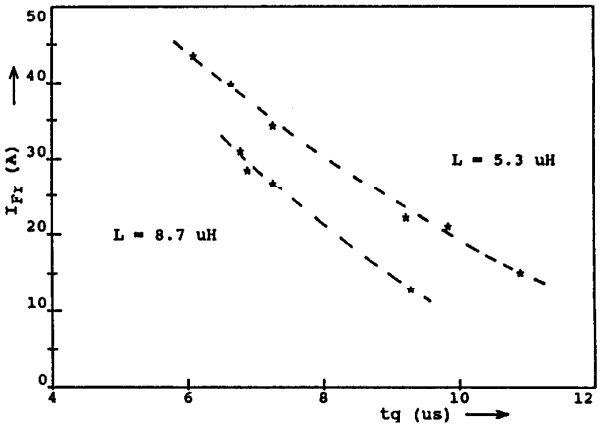

Figure 11: Forward recovery current of the GTO in mode 1 as a function of t_q. I_{Tpu} = 300 A, C = 6.9 µF, V_C variable

Figure 11 also shows that the device can be used at t_q down to 6 µs without danger of accidental turn-on.

The amount of charge that flows out of the gate into the gate drive is important for the power rating of the gate unit. This charge depends on the time where the negative gate signal is applied. The gate current was measured in ZCS mode 2 for different time intervals T_1 between

the start of the current fall (I_T = 90% I_{Tpk}) and the begin of the negative gate current.

Figure 12 presents the anode current at T_1 = 5.5 µs. Note that anode current and gate current are almost equal during the hold-off time. When the anode voltage rises, a displacement current is seen in both current waveforms. The gate charge for different values of T_1 is plotted in fig. 13. Both Q_g (the charge extracted from the gate before the maximum gate current is reached) and Q_{gtot} (the total amount of charge flowing out of the gate of the GTO)

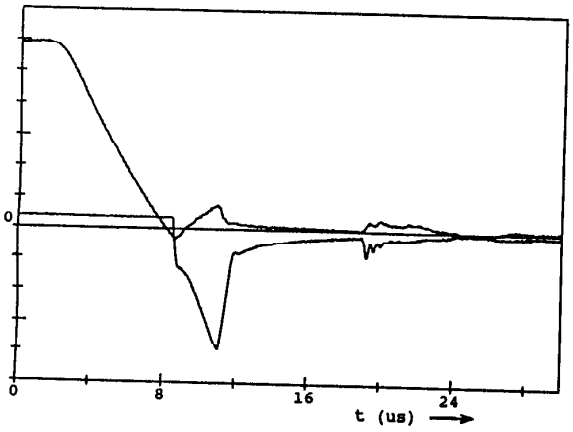

Figure 12: Anode current and gate current of the GTO in mode 2.
I_T : 50 A/div, I_G : 10 A/Div

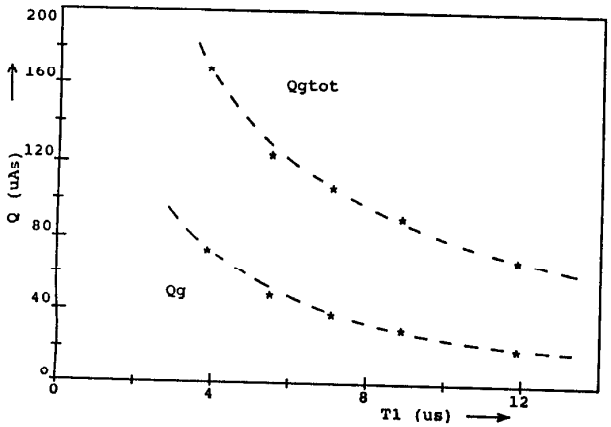

Figure 13: Gate charge in mode 2 as a function of the time when the negative gate current is applied. I_{Tpk} = 300 A, L = 5.3 µH, C = 10.2 µF, V_C = 450 V

decrease exponentially. The power needed for the reverse gate drive can be estimated to

$$P_g = f \cdot Q_{gtot} \cdot V_{Gkx} \leq 3W/kHz \qquad (5)$$

at I_{Tpk} = 300 A. This small amount of gate drive power is an important benefit of ZCS with GTOs. For instance at 10 kHz, only 30 W of reverse gate power would be necessary.

The switching losses have been investigated in all the different ZCS modes. For a given set of L and C, the turn-off losses in mode 1 and 2 are shown in fig. 14 as a function of dI/dt of the anode current. It is not surprising that a reverse blocking GTO used in mode 1 shows the largest amount of switching losses, because a large portion of the losses is generated during the reverse recovery. This portion increases with dI/dt because a larger dI/dt is obtained from a higher commutation voltage V_C (see fig. 4). When the GTO is unbedded in a switch as shown in fig. 3, losses occur only when the

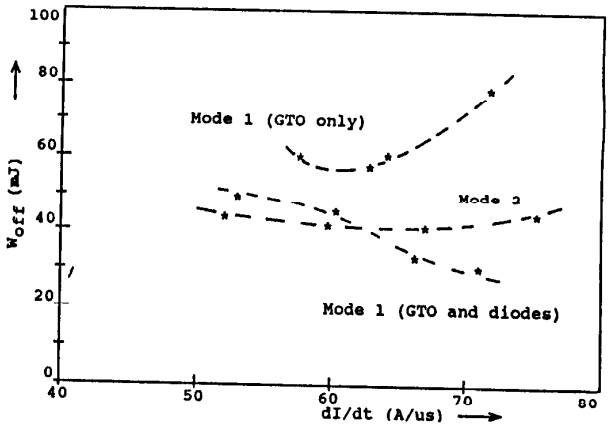

Figure 14: Switching losses of the GTO in ZCS modes 1 and 2 as a function of dI/dt. I_{Tpk} = 300 A, L = 5.3 µH, C = 6.9 µF, V_C variable

voltage rises. Here the losses are lower at large values of dI/dt because the hold-off time increases almost proportionally to dI/dt. The losses in mode 2 are found to be almost constant. This is because there is a larger step in the forward blocking voltage when the commutation voltage is larger. Thus two effects (larger t_q, larger voltage step) compensate each other.

In ZCS mode 4, the turn-off losses were investigated as a function of the equivalent pulse frequency, the hold-off interval, and the start or the negative gate current. Surprisingly the losses were almost constant during all the experiments. Although the equivalent pulse frequency was varied between 8 kHz and 22 kHz, the hold-off time between 2 µs and 10 µs and the start of the negative gate current through the complete range of the hold-off time, a significant dependance of the losses on one of these parameters could not be found.

The turn-off losses were 18 mJ at 10 kHz and 21 mJ at 20 kHz. This is only half of the losses obtained in ZCS modes 1 and 2.

The most remarkable result, however, is the switching loss in ZCS mode 3 when the GTO is used in the configuration of fig. 3. At a current amplitude of 300 A, an equivalent pulse frequency of 20 kHz, and hold-off times of approximately 6 μs, the turn-off losses are as low as 5 mJ. This is only one quarter of the losses in mode 4 and about one eight of the losses in modes 1 and 2. The explanation for these very good results is found in the short duration of the peak current, the smooth decrease of anode current, and the soft rise of anode voltage.

It can be stated without any doubts that the ZCS mode 3, which is obtained in the resonant DC current link inverter, is the most convenient zero current switching mode for a GTO.

4 Behaviour of SCRs in a New Zero Current Switching Mode

The investigation of the switching behaviour of GTOs under ZCS revealed that the operation mode 3 in fig. 2 is very convenient for a GTO. The effects of stored charge that usually lead to long switching times and high losses are widely reduced due to the smooth shape of current and reapplied forward voltage. It is very likely that also an SCR may benefit from this new ZCS mode. Therefore the behaviour of SCRs in the RDCCLI was also investigated.

A test circuit according to fig. 15 was set up in order to simulate the waveforms typical for a RDCCLI in continuous operation. In this circuit, the current source is realized by the large inductance L_d (45 mH). When T_1 and T_2 are off, the current source charges the capacitor C linearly. The resonant current cycle is started by turning on either T_1 or T_2. The sinusoidal current pulse is flowing via L, C, T_1 and $V_d/2$ or T_2 and $V_d/2$. The current in L_d increases when T_1 is switched and decreases when T_2 is switched. This provides efficient control on the current I_{Ld}. V_d was chosen at 230 V, L at 61 μH and C at 500 nF and 900 nF, so that two different frequencies were realized.

When only I_{Ld} is changed and the time intervals between two pulses are kept constant, the amplitudes of the current and voltage waveforms change proportionally to I_{Ld}, while the timing and shape of the pulses is constant. Of course also dI/dt and dV/dt are changed proportionally.

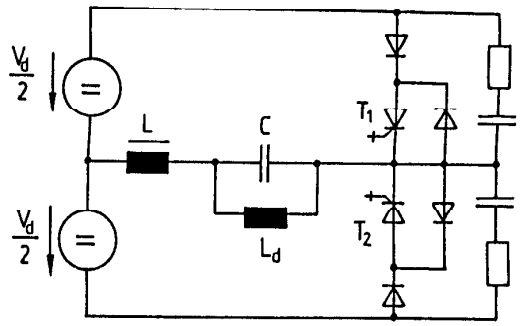

Figure 15: Test circuit for ZCS mode 3 in continuous operation

A symmetrical fast turn-off thyristor IR 81RM100 rated at 125 A RMS and 1000 V was used instead of the GTO switches and diodes in fig. 15. Peak currents between 30 A and 115 A were obtained at pulse frequencies of 20 kHz and 27 kHz. For the lower frequency, a constant reverse recovery time of only 1.5 μs at a peak reverse recovery current of less than 2 A was measured over the complete peak anode current range. The hold-off time during which the device is kept in the reverse blocking state could be reduced to only 6 μs, while the data sheet specification of t_q was 20 μs.

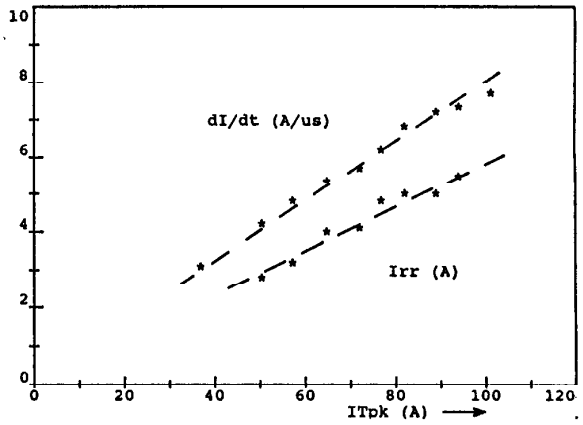

Figure 16: Reverse recovery current I_{rr} of SCR 81RM100 and dI/dt of the anode current waveform as a function of the peak anode current I_{Tpk}

For the higher frequency, the reverse recovery time t_{rr} was constant at 2 μs approximately, while the peak reverse recovery current I_{rr} changed as indicated in fig. 16. The figure also shows how dI/dt is rising proportionally with the current amplitude I_{T1pk}. The hold-off time was again as low as 6 μs over the complete range

of currents. The rate of rise of the reapplied voltage was 50 V/μs in the worst case. These results were obtained without any negative voltage across the gate during turn-off.

In both cases the turn-on losses were seen to be very small, below 1 mJ in all the cases, and the turn-off losses were even smaller and could hardly be measured.

The reason for the extremely good behaviour of the SCR in this new application is the very large inductance in series with the device, and the slow decrease of current prior to turn-off. The latter allows the stored charge almost to follow the instantaneous current level and thus to have only few charge stored in the base regions when turn-off occurs. This and the large inductance helps to keep the forward recovery current very small, so that the device is not turned on again although the forward recovery current is flowing completely via the gate-cathode junction.

5 Conclusion

The application of GTOs in different modes of zero current switching was investigated. It is possible to achieve hold-off times much smaller than for thyristors if the GTO is used in combination with an antiparallel diode. In ZCS modes with trapezoidal current, the switching losses can be widely reduced if the hold-off time is several microseconds long. In that case, an increase in switching frequency over the limits for GTOs and for thyristors is possible. The operation conditions are much more convenient for a GTO in the case of sinusoidal current. The application where the device stresses during the switching transitions are smallest is the Resonant DC Current Link Inverter. Here turn-on and turn-off losses are very small, even for very short hold-off times, and the switching frequencies can be pushed far above the limitaions known so far. The drawback is that a series diode has to be used in order to attain a reverse blocking switch. This increases both the number of devices and the conduction losses of the switch.

An additional investigation was carried out on the behaviour of SCRs in the RDCCLI. In this application, the device can be used with hold-off intervals much shorter than the specified t_q.

However, a GTO still has the advantage of shorter hold-off times that can even be reduced down to zero. The selection of a device for a zero current switching application is thus a trade-off between high frequency and low conduction loss and complexity.

Acknowledgement

We would like to thank Mr. Frank Ransmann for carrying out a lot of the experimental work reported in this paper.

References:

[1] S. M. Tenconi, M. Zambelli, L. Malesani, P. Tenti: "The reverse blocking GTO as a very fast turn-off thyristor", Proc. of IEEE-IAS Ann. Meeting 1986, pp. 377-383

[2] L. Malesani, P. Tenti: "Medium frequency GTO inverter for in-duction heating applications", Proc. of EPE 1987, pp. 271-276

[3] Thomson Semiconductors, 1987: "ZTO: A new high power component", "ZTO: New perspectives for high power conversion", "Optimal use of a ZTO", Application Notes

[4] Marconi Electronic Devices, 1987: "The ZTO zero turn-off thyristor", Application Notes

[5] C. Millour, J.P. Abgrall, 1988: "New perspectives for power converters with ZTO thyristors", Application Notes

[6] K.E. Bornhardt: "Switching behaviour of a pulse-commutated GTO", Proc. of IEE-PEVD 1988, London, pp. 83-86

[7] J.P. Pascal, G. Coquery, R. Lallemand: "Increasing frequency using GTO in gate-assisted turn-off mode", Proc. of IEE-PEVD 1988, London, pp. 87-90

[8] Y. Murai, T. Lipo: "High frequency series resonant DC link power conversion", Proc. of IEEE-IAS Ann. Meeting 1988, pp. 648-656

[9] A. Mertens, H.-Ch. Skudelny: "Switching losses in a GTO inverter for induction heating", Proc. of IEEE PESC '89, Milwaukee, pp. 91-98

[10] A. Mertens, H.-Ch Skudelny: "Operation and control requirements for a GTO used in a parallel resonant inverter for induction heating", Proc. of EPE 89, Aachen, pp. 1097-1102

[11] L. Malesani, R.J. Morris: "Design and characterization of GTO devices for medium frequency applications", Proc. of EPE 1989, Aachen, pp. 115-120

[12] R.J. Morris, F.J. Wakeman, "A new family of GTO devices for medium frequency applications", Proc of IEEE-IAS Ann. Meeting 1989, San Diego, pp. 1264-1269